

CHAPTER V. Triggering, feedback, and shutting off of AGN activity

AGN fueling and feedback

Francoise Combes

Observatoire de Paris, LERMA, Collège de France, CNRS, PSL University,
Sorbonne University, UPMC, Paris
email: francoise.combes@obspm.fr

Abstract. Dynamical mechanisms are essential to exchange angular momentum in galaxies, drive the gas to the center, and fuel the central super-massive black holes. While at 100pc scale, the gas is sometimes stalled in nuclear rings, recent observations reaching ~ 10 pc scale have revealed, within the sphere of influence of the black hole, smoking gun evidence of fueling. Observations of AGN feedback are described, together with the suspected responsible mechanisms. Molecular outflows are frequently detected in active galaxies with ALMA and NOEMA, with loading factors between 1 and 5. When driven by AGN with escape velocity, these outflows are therefore a clear way to moderate or suppress star formation. Molecular disks, or tori, are detected at 10pc-scale, kinematically decoupled from their host disk, with random orientation. They can be used to measure the black hole mass.

Keywords. galaxies: active, galaxies: general, galaxies: nuclei, galaxies: Seyfert, galaxies: spiral

1. Introduction: the main paradigm

For a long time, the main unification paradigm to explain the large variety of AGN, and in particular the type 1 with broad lines (BLR), and the type 2, with only narrow lines (NLR), has been the obscuration of the accretion disk by a dusty torus, hiding the BLR and showing only the NLR to the observer (Urry & Padovani 1995). This idea is still valid for a certain number of AGN (for instance type 2 Seyfert which reveal their BLR in polarized light), but is known not to be the only parameter distinguishing the various AGN, since there exist intrinsic differences between Sy1 and Sy2, and also a number of changing look AGNs have been discovered, while their transformation from Sy1 to Sy2 and vice-versa in time-scales of dozens of years has nothing to do with obscuration (Denney *et al.* 2014; McElroy *et al.* 2016).

In the last decade, high spatial resolution observations in the mid-infrared with the VLT Interferometer (VLTI) showed that the dust on parsec scales is not mainly in a thick torus, but instead in a polar structure, forming like a hollow cone, perpendicular to a thin disk (e.g., Asmus *et al.* 2016; Hönig 2019) and references therein). A large majority of objects ($\sim 90\%$) reveal that most ($>50\%$) of the mid-infrared emission of the dust comes from a polar structure, leaving little room for a torus contribution (Asmus 2019). The new view which is sketched now for the cold gas is a two component medium, one inflowing in a thin disk, where millimeter lines have been found, with also H₂O masers, or the rotational lines of warm H₂, and an outflowing component, in the perpendicular direction, responsible for the polar dust emission. Molecular outflows will be driven along the borders of this hollow cone. The inner boundary of the dusty thin disk would correspond to the sublimation of the dust by the AGN radiation. The circum-nuclear molecular disk could be observed to extend down to smaller distances from the center.

In the following, I review recent observations at high-angular resolution of the molecular gas, showing how gravity torques can help feeding the central black hole, through

exchange of angular momentum. These are the consequences of nuclear dynamical features, such as nuclear bars & spirals. The same observations might reveal outflows, occurring simultaneously with inflow, albeit in different directions. These outflows are due to the feedback effect of the AGN, added to the star formation feedback. Frequently in nearby active galaxies, molecular circum-nuclear disks are observed; with decoupled kinematics from the larger-scale galactic disks. These parsec-scale structures may be identified to molecular tori, able to obscure the central accretion disks. Being within the sphere of influence of the black holes, they help to determine their mass.

2. Nuclear trailing spirals

Observed nuclear spirals bring clear evidence of fueling. They were detected first in NGC 1566 (Combes *et al.* 2014), during the first ALMA observations, with 0.5 arcsecond ~ 25 pc resolution. In this barred spiral, there is an $r = 400$ pc ring, corresponding to the inner Lindblad resonance (ILR) of the bar. The stellar periodic orbits, which attract all regular orbits, change by 90° at each resonance (Contopoulos & Papayannopoulos 1980). They are parallel to the bar inside corotation, and become perpendicular in-between the two ILRs.

The gas behaviour may be derived from these orbits; the gas elliptical streamlines tend to follow them, but gas clouds are subject to collisions. The ellipses are gradually tilted by 90° and wind up in spiral structures. The precession rate of these elliptical orbits in the epicyclic approximation is equal to $\Omega - \kappa/2$, with Ω the rotation frequency $= V/r$, and κ being the epicyclic frequency. When the dissipative gas is driven to the center, the precession rate first increases, since $\Omega - \kappa/2$ increases, and the spiral is trailing. But inside the ILR, the precession rate reaches a maximum and declines, and this changes the winding sign of the gas, which is expected to be in a leading spiral. The reversal of the winding sense has also the consequence of reversing the sign of the gravity torques exerted by the stellar bar on the gas (Buta & Combes 1996). The torque is negative from corotation to ILR, but then is positive inside the ILR, this confines the gas in the ILR ring, where it forms stars actively.

However, in the presence of the central black hole, all frequencies Ω and $\Omega - \kappa/2$ increase again towards the center, as shown in Fig. 1. This is able to reverse the winding sense of the gas spiral, if a sufficient amount of gas is within the influence of the black hole. In that case, the gravity torques become negative again, and the gas is driven to the center, to fuel the AGN. The very presence of a nuclear trailing spiral is smoking gun evidence of the AGN fueling.

Such trailing nuclear spirals have been found also in NGC 613 (Audibert *et al.* 2019) and in NGC 1808 (Audibert *et al.* 2020, in prep.), as can be seen in Fig. 1. The nuclear spiral is conspicuous in the CO(3-2) emission line, but also in the dense gas tracers like HCN, HCO⁺ or CS. The rotation curves of these galaxies, derived both from the stellar potential (traced by near-infrared images) and the observed kinematics of the gas, confirm that the nuclear gas is falling within the sphere of influence of the black holes.

The gravity torques have been measured on the deprojected images of the molecular gas, with the method described in Garcia-Burillo & Combes (2012), and the torques are indeed negative (Audibert *et al.* 2019). The computation allows to quantify the strength of the torques, and shows that the gas loses most of its angular momentum in one rotation, i.e. 10 Myr.

3. Molecular outflows

In some cases, molecular outflows are observed simultaneously with the evidence of fueling. This is the case of NGC 613, where a very short (23pc) and small velocity

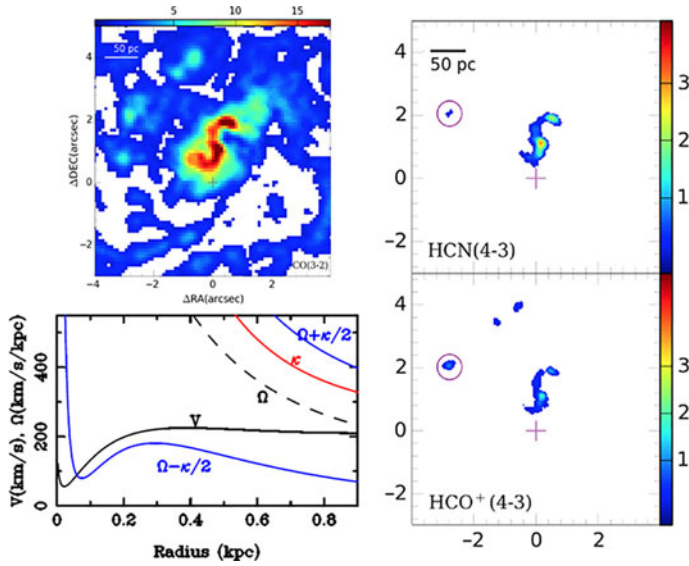


Figure 1. ALMA observations of the Seyfert-2 galaxy NGC 1808. Left is a zoomed $4'' \times 4''$ region of the CO(3 – 2) intensity map, showing the nuclear trailing spiral. Right are the intensity maps of the dense gas tracers HCN(4 – 3) and HCO⁺(4 – 3). The size is given in parsec by the 50pc bar. At the bottom left, is the model rotation curve, taken from both the near-infrared (potential from old stars) and the gas observed velocity (Salak *et al.* 2016). From Audibert *et al.* (2020) in prep., and Combes *et al.* (2019).

(300km/s) outflow is detected on the minor axis, in the same direction of the radio jet, mapped at cm wavelength with the VLA (Audibert *et al.* 2019). This was possible thanks to the ALMA resolution of 60 mas (5pc). The coincidence with the radio jet strongly suggests that the outflow is AGN feedback in the radio mode.

In other cases (e.g. NGC 1566) no molecular outflow is detected. In NGC 1808, an outflow has been known for a long time, at large scale, from ionized gas and dust ejected perpendicular to the plane, creating an extra-planar medium (Busch *et al.* 2017). However, at parsec scale, the CO emission from ALMA does not reveal any outflow. In that case, it can be concluded that the outflow is driven by supernovae feedback, but not from the AGN.

In that NGC 1808 galaxy, the starburst and AGN contributions can be distinguished by the diagnostics of line ratios between HCN and HCO⁺ or CS. Close to the AGN, the HCN line is considerably enhanced (Usero *et al.* 2004; Krips *et al.* 2008), due to the X-rays from the AGN.

In these nearby low-luminosity AGN, the main mechanism to drive molecular outflows is entrainment by the radio jets. There are two main modes identified for AGN feedback:

- the quasar mode, or radiative mode with winds. This occurs when the AGN luminosity is close to the Eddington luminosity, for young quasars at high redshift essentially. Then the radiation pressure exerted on the ionized gas (with the Thomson cross-section) can drive an ionized wind. A similar effect can occur with the radiation pressure on dust, with a higher cross-section.

- the radio mode, or kinetic mode, due to radio jets. This occurs when the AGN luminosity is lower than 1/100 th of the Eddington luminosity, typically at low redshift. Massive galaxies, and early-type galaxies are frequently the host of radio-loud AGN. These low-luminosity AGN are radiatively inefficient (ADAF). In the low redshift universe, strong AGN feedback in the radio mode is observed frequently in cooling flows of galaxy clusters.

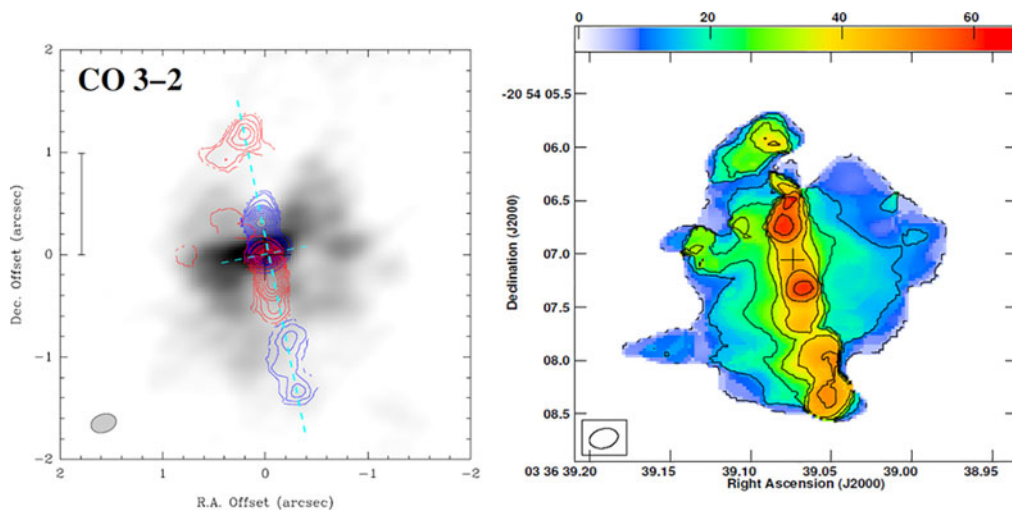


Figure 2. ALMA CO(3-2) map of the galaxy NGC 1377: Left, the grey-scale corresponds to the emission close to systemic velocity, while the high velocity (80 to 150 km/s from V_{sys}) is indicated as red and blue for red-shifted and blue-shifted emission respectively. The vertical bar indicates a scale of 100 pc. The dashed line indicates the jet axis (and nuclear disk) orientations. Right: the velocity dispersion (moment 2) map, from 0 to 66 km/s. The cross indicates the position of the continuum peak at 345 GHz. From [Aalto *et al.* \(2016\)](#).

There is a radio-mode molecular outflow in the proto-typical Seyfert 2 galaxy NGC 1068. The nucleus is off-centered, and the radio jet is not perpendicular to the plane; therefore it is sweeping out some gas in the disk ([Garcia-Burillo *et al.* 2014](#)). The molecular outflow is estimated at $63M_{\odot}/\text{yr}$, or 10 times the star formation rate in the central region.

In NGC 1068, the high resolution of ALMA has allowed the detection of a molecular torus, with both the CO(6–5) emission line, and with the dust emission at $432\mu\text{m}$. The radius of the torus depends on the tracer, it is with CO(6–5) 5–6 pc, but larger in low-J lines, like CO(2–1). The various tracers yield different aspects of the cold medium in the center. The CO disk is warped, and appears more inclined than the H_2O maser disk ([Garcia-Burillo *et al.* 2016](#)). It is possible that the circum-nuclear disk is unstable, through the Papaloizou-Pringle instability ([Papaloizou & Pringle 1984](#)).

The molecular torus is located just at the base of a polar dusty cone. The cone has been mapped in the near-infrared, with SPHERE on the VLT, and in particular the polarisation is revealing beautifully the conical structure ([Gratadour *et al.* 2015](#)).

The radio mode might also be at play in the lenticular galaxy NGC 1377, although no radio jet has been detected, and the galaxy is the most radio-quiet found, in terms of the radio-far-infrared correlation. A weak radio emission is detected at the center, but much weaker than expected from the well known correlation ([Helou *et al.* 1985](#)).

As shown in [Fig. 2](#), ALMA has detected in this galaxy a very narrow molecular outflow ([Aalto *et al.* 2016](#)). The molecular outflow changes sign along the flow, on each side of the galaxy. This very surprising behaviour is very rare, and is interpreted as the precession of the jet, which happens to be very little inclined on the sky plane. Therefore a precession of 10° only is sufficient to reverse the sign of the flow velocity towards the observer. Such precession is observed in micro-quasars jets in the Milky Way, for instance SS433 ([Mioduszewski *et al.* 2005](#)).

The molecular gas in the cone is derived to be $10^8 M_{\odot}$, and there is $10^7 M_{\odot}$ in the outflow ([Aalto *et al.* 2016](#)). A model of a precessing molecular outflow has been

Table 1. Radii, masses, and inclinations of the molecular tori

Galaxy	Radius (pc)	M(H ₂) 10 ⁷ M _⊙	inc(°) torus	PA(°) torus	inc(°) gal
NGC 613	14±3	3.9±1.4	46±7	0±8	36
NGC 1326	21±5	0.95±0.1	60±5	90±10	53
NGC 1365	26±3	0.74±0.2	27±10	70±10	63
NGC 1433	–	–	–	–	67
NGC 1566	24±5	0.88±0.1	12±12	30±10	48
NGC 1672	27±7	2.5±0.3	66±5	0±10	28
NGC 1808	6±2	0.94±0.1	64±7	65±8	84
NGC 1068	7±3	0.04±0.01	80±7	120±8	24

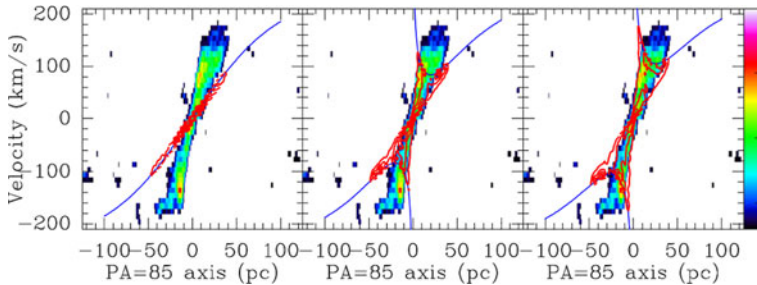


Figure 3. ALMA CO(3-2) observations of the galaxy NGC 1672. The 3 panels are the position-velocity diagrams in color, along the major axis of the molecular disk (or torus), with superposed in red, three models with different values of the central black hole mass (0, 2.5 and 5.0 10⁷ M_⊙). The predicted circular velocity is reproduced in blue lines. From [Combes *et al.* \(2019\)](#).

found compatible with the data. The velocity of the flow, according to the model, ranges between 250 and 600 km/s. The flow is launched at a distance from the center lower than 10 pc. It cannot be driven by supernovae feedback, since there is no starburst in the galaxy, and the flow would not be so collimated. A radio jet must exist at a low level, or has existed in a recent past.

4. Molecular tori

When the high-angular resolution is available with ALMA, the frequency of detection of molecular tori in nearby Seyfert galaxies is quite high, 7 out of 8, as shown in the Table 1.

We call "molecular torus" the circum-nuclear molecular disk, of parsec scale, which is kinematically and spatially decoupled from the rest of the disk. It might not appear as a torus, except in favorable cases, like in NGC 1365. The molecular tori are located within the sphere of influence of the black holes, and can serve to measure their mass. The example of the Sy2 NGC 1672, where the torus is seen almost edge-on, is displayed in Fig. 3. The ALMA resolution is 3 pc. The position-velocity diagram reveals a strong velocity gradient of about 180 km/s in 30 pc.

A 3D modelisation of the dynamics of the nuclear disk has led to a black hole mass of 5 10⁷ M_⊙ ([Combes *et al.* 2019](#)). The black hole mass determination from the gas kinematics is a precious method, for these low-luminosity AGN, which are late-type spiral galaxies frequently with a pseudo-bulge. For them the scaling relation between the central velocity dispersion and the mass of their black hole is quite scattered (e.g., [Graham *et al.* 2011](#)). This is not the case of more massive early-type galaxies, where the gas method has also been used with success ([Davis *et al.* 2018](#)).

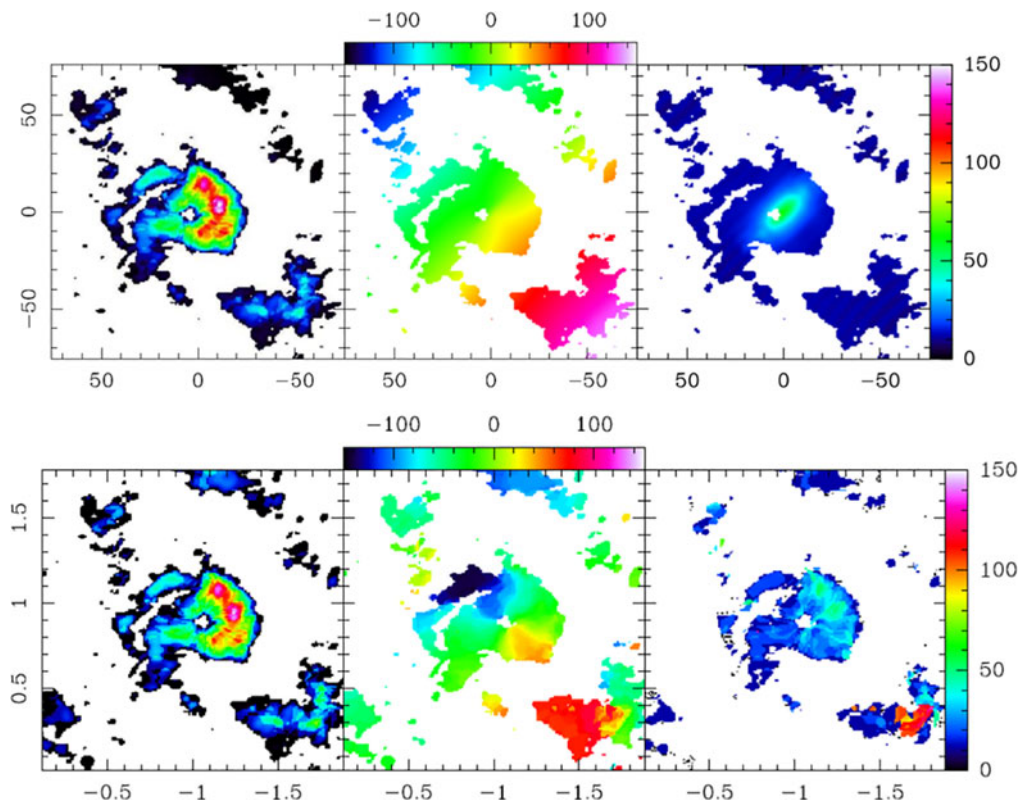


Figure 4. ALMA CO(3-2) observations of the galaxy NGC 1365. In each row, the three panels display the three first moments (intensity, velocity and dispersion). The velocity color scale is in km/s. The model corresponds to a black hole mass of $4 \times 10^6 M_{\odot}$. Top is the model, and bottom the observations. The scale is spatial offset in parsec for the model, and in arcsec for the observations.. From [Combes *et al.* \(2019\)](#).

The 3D modelisation of the molecular torus dynamics for the Sy 1.8 galaxy NGC 1365 is displayed in Fig. 4. The black hole mass is $4 \times 10^6 M_{\odot}$ ([Combes *et al.* 2019](#)).

One common feature to the detected molecular tori, is their random orientation and decoupling with the large-scale disk of their host, cf Table 1. This feature is not unexpected, given the very different time-scales at parsec scale and kpc-scales, and the almost spherical potential of the central galaxy at small scale. The material near the black hole will eventually inflow and fuel the AGN, and will be replaced by accreted gas, coming with different orientations and angular momenta. Numerical simulations show examples of central starbursts, where gas is ejected in a fountain through supernovae feedback, and may cool and fall back with random orientation, sometimes in a polar ring ([Renaud *et al.* 2015](#); [Emsellem *et al.* 2015](#)).

Examples of nuclear disks decoupled from their host disks are frequently seen, as in the Milky-Way, where a circum-nuclear ring of 2-3pc in radius surrounds an almost face-on mini-spiral, or in NGC 4258, where anomalous arms (in fact the radio jet) are winding in the plane of the large-scale disks, with the normal spiral arms.

In the edge-on disc galaxy HE1353-1917, [Husemann *et al.* \(2019\)](#) have found a radio jet impinging the molecular gas of the host, and producing an outflow; in addition, [OIII] emission in a cone oriented at only $\sim 10^{\circ}$ from the edge-on plane, reveals gas illuminated by the AGN, collimated by a highly inclined torus.

5. Summary

Recent high spatial resolution observations with ALMA have revealed the role played by dynamical features like bars to drive the gas at parsec scales, and fuel the AGN. The process is occurring in several steps, first from corotation, the gas is driven inwards, and piles up in a ring at the inner Lindblad resonance, at 100 pc-scale. Then, either through a nuclear bar, or through dissipation, the gas may be driven further in; there, within the sphere of influence of the black hole, it rapidly loses its angular momentum, settles in a 10pc-scale disk or torus and fuels the AGN.

Simultaneously, the AGN feedback through radiative or radio mode, according to the Eddington ratio, may drive molecular outflows, in a perpendicular direction. In some cases, the feedback is from the supernovae of a central starburst, in association (or not) to the AGN feedback. The AGN feedback can have a strong coupling with the gas in the host disk, due to the mis-alignment of the nuclear and large-scale disks.

Circum-nuclear disk, or molecular tori are frequently detected in nearby Seyferts, with a random orientation, kinematically decoupled from their host disk. This mis-alignment between small scales and large scales is due to random gas accretion, and different dynamical time-scales.

References

- Aalto, S., Costagliola, F., Muller, S., *et al.* 2016, *A&A*, 590, A73
 Asmus, D. 2019, *MNRAS*, 489, 2177
 Asmus, D., Höning, S. F., Gandhi, P., *et al.* 2016, *Ap. J.*, 822, 109
 Audibert, A., Combes, F., Garcia-Burillo, S., *et al.* 2019, *A&A*, in press., [arXiv:1905.01979](https://arxiv.org/abs/1905.01979)
 Busch, G., Eckart, A., Valencia-S, M., *et al.* 2017, *A&A*, 598, A55
 Buta, R. & Combes, F. 1996, *Fund. Cosmic Phys.*, 17, 95
 Combes, F., Garcia-Burillo, S., Casasola, V., *et al.* 2014, *A&A*, 565, A97
 Combes, F., Garcia-Burillo, S., Audibert, A., *et al.* 2019, *A&A*, 623, A79
 Contopoulos, G. & Papayannopoulos, T. 1980, *A&A*, 92, 33
 Davis, T. A., Bureau, M., Onishi, K., *et al.* 2018, *MNRAS*, 473, 3818
 Denney, K. D., De Rosa, G., Croxall, K., *et al.* 2014, *Ap. J.*, 796, 134
 Emsellem, E., Renaud, F., Bournaud, F., *et al.* 2015, *MNRAS*, 446, 2468
 Garcia-Burillo, S. & Combes, F. 2012, *JPhCS*, 372, a2050
 Garcia-Burillo, S., Combes, F., Usero, A., *et al.* 2014, *A&A*, 567, A125
 Garcia-Burillo, S., Combes, F., Ramos Almeida, C., *et al.* 2016, *Ap. J.*, 823, L12
 Graham, A. W., Onken, C. A., Athanassoula, E., & Combes, F. 2011, *MNRAS*, 412, 2211
 Gratadour, D., Rouan, D., Grosset, L., *et al.* 2015, *A&A*, 581, L8
 Helou, G., Soifer, B. T., Rowan-Robinson, M., *et al.* 1985, *Ap. J.*, 298, L7
 Höning, S. F., 2019, *Ap. J.*, 884, 171
 Husemann, B., Scharwächter, J., Davis, T. A., *et al.* 2019, *A&A*, 627, A53
 Krips, M., Neri, R., Garcia-Burillo, S., *et al.* 2008, *Ap. J.*, 677, 26
 McElroy, R. E., Husemann, B., Croom, S. M., *et al.* 2016, *A&A*, 593, L8
 Mioduszewski A. J., Dhawan, V., Rupen, M. P., *et al.* 2005, *ASPC*, 340, 281
 Papaloizou, J. C. B. & Pringle, J. E. 1984, *MNRAS*, 298, 721
 Renaud, F., Bournaud, F., Emsellem, E., *et al.* 2015, *MNRAS*, 454, 3299
 Salak, D., Nakai, N., Hatakeyama, T., Miyamoto, Y., *et al.* 2016, *Ap. J.*, 823, 68
 Urry, C. M. & Padovani, P. 1995, *PASP*, 107, 803
 Usero, A., Garcia-Burillo, S., Fuente, A., *et al.* 2004, *A&A*, 419, 897